

Topological susceptibility and axion potential in two-flavor superconductive quark matter

Fabrizio Murgana^{1,2,*} David E. Alvarez Castillo^{3,4,5,†} Ana G. Grunfeld^{6,7,‡} and Marco Ruggieri^{1,2,§}

¹*Department of Physics and Astronomy “Ettore Majorana,”*

University of Catania, Via Santa Sofia 64, I-95123 Catania, Italy

²*INFN-Sezione di Catania, Via Santa Sofia 64, I-95123 Catania, Italy*

³*Institute of Nuclear Physics, Polish Academy of Sciences, Radzikowskiego 152, 31-342 Cracow, Poland*

⁴*Incubator of Scientific Excellence—Centre for Simulations of Superdense Fluids,*

University of Wrocław, plac Maksa Borna 9, PL-50204 Wrocław, Poland

⁵*Facultad de Ciencias Físico Matemáticas, Universidad Autónoma de Nuevo León, Avenida Universidad S/N, Ciudad Universitaria, 66455 San Nicolás de los Garza, Nuevo León, Mexico*

⁶*CONICET, Godoy Cruz 2290, C1425FQB Ciudad Autónoma de Buenos Aires, Argentina*

⁷*Departamento de Física, Comisión Nacional de Energía Atómica,*

Avenida Libertador 8250, C1429 BNP, Ciudad Autónoma de Buenos Aires, Argentina



(Received 6 May 2024; accepted 28 June 2024; published 29 July 2024)

We study the potential of the axion, a , of Quantum Chromodynamics, in the two-flavor color superconducting phase of cold and dense quark matter. We adopt a Nambu-Jona-Lasinio-like model. Our interaction contains two terms, one preserving and one breaking the $U(1)_A$ symmetry: the latter is responsible of the coupling of axions to quarks. We introduce two quark condensates, h_L and h_R , describing condensation for left-handed and right-handed quarks respectively; we then study the loci of the minima of the thermodynamic potential, Ω , in the (h_L, h_R) plane, noticing how the instanton-induced interaction favors condensation in the scalar channel when the θ angle, $\theta = a/f_a$, vanishes. Increasing θ we find a phase transition where the scalar condensate rotates into a pseudoscalar one. We present an analytical result for the topological susceptibility, χ , in the superconductive phase, which stands both at zero and at finite temperature. Finally, we compute the axion mass and its self-coupling. In particular, the axion mass m_a is related to the full topological susceptibility via $\chi = m_a^2 f_a^2$; hence our result for χ gives an analytical result for m_a in the superconductive phase of high-density Quantum Chromodynamics.

DOI: [10.1103/PhysRevD.110.014042](https://doi.org/10.1103/PhysRevD.110.014042)

I. INTRODUCTION

Axions, originally proposed by Peccei and Quinn in 1977 as a possible solution to the strong CP problem in Quantum Chromodynamics (QCD) [1–9], have since then become prime candidates for dark matter [3, 10–19]. The quest to understand the nature of dark matter, which constitutes a significant portion of the mass of the Universe, has led to extensive theoretical and experimental efforts, with axions emerging as particularly compelling candidates due to their unique properties. Theoretical

models and experiments constrain the axion mass to be very light, on the order of 10^{-6} to 10^{-3} eV [20]. This range arises from considerations such as the possible violation of the CP symmetry of QCD and the consequent electric dipole moment for the neutron [21–28], astrophysical and cosmological observations, and experimental searches for axions using techniques like cavity haloscopes and axion helioscopes. In addition to their potential role as dark matter candidates, axions, behaving as scalar fields, may also serve as the constituents of boson stars [29] and arrange into axion stars [30–44] and form Bose-Einstein condensates [45, 46]; see also [47, 48] for further astrophysical applications.

Furthermore, not only axions but axionlike particles have been proposed to play the role of dark matter in order to account for missing matter at cosmological scales. It has been speculated that axions may exist in compact star interiors, and can be buried deep in their cores, giving rise to interaction with quark matter, as we investigate in this study. In the assumption that axions may be able to escape

*Contact author: fabrizio.murgana@dfa.unict.it

†Contact author: dalvarez@ifj.edu.pl

‡Contact author: ag.grunfeld@conicet.gov.ar

§Contact author: marco.ruggieri@dfa.unict.it

Published by the American Physical Society under the terms of the [Creative Commons Attribution 4.0 International license](https://creativecommons.org/licenses/by/4.0/). Further distribution of this work must maintain attribution to the author(s) and the published article’s title, journal citation, and DOI. Funded by SCOAP³.

compact star interiors, they would be prone to interact with magnetic fields via the so called Primakov effect, i.e., the axion resonantly converting into a radio photon [49,50], which would provide a feasible way to detect them. The emission of axions could also cool compact stars, deviating their thermal evolution from standard scenarios [51–54].

Macroscopic properties of compact stars bearing axions have been presented in [55,56], where particular modeling has resulted in unstable compact stars that would collapse due to radial oscillations if vector repulsive interactions in quark matter are not taken into account. Furthermore, axions have been investigated within astrophysical contexts, particularly in relation to supernova explosions and the formation of protoneutron stars [57,58]. Previous works on the coupling of the QCD axion to quarks can be found in [55,59–69], where in particular the effect of the QCD chiral phase transition on the low-energy properties of the axion itself has been investigated, both at finite temperature and at finite quark chemical potential, μ . The axions enter the model similarly to the θ angle of QCD; in fact, formally one can pass from QCD at finite θ to QCD with a finite axion background by identifying $\theta = a/f_a$, where a denotes the axion field and f_a is the axion decay constant. Therefore, studies of the QCD interaction with axions at finite chemical potential serve as studies of quark matter at finite θ and finite μ as well. Hence, within our work we will interchangeably use θ in place of a/f_a .

Deep within the dense cores of compact stars, where matter is subjected to extreme pressures and temperatures, exotic phases of strongly interacting matter come into play, as the 2SC color superconductive phase [60,70–73]. This phase is characterized by a nonvanishing quark-quark condensate: as such, it is not a color singlet, transforming as a color antitriplet under color rotations. In most previous calculations, in particular in those related to the QCD phase diagram, only the scalar condensate was considered, as it is the one that is favored by the one-instanton exchange. Within the present work, we introduce both a scalar and a pseudoscalar condensate, since both of them are relevant when the coupling to the axions is considered. In agreement with the common lore, we show that our model is consistent with favoring the scalar condensate when the axion is not included in the model. On the other hand, changing θ can result in a phase transition to a new ground state where the condensate is a pseudoscalar one, in qualitative agreement with previous studies in normal quark matter [55,65–68]. Therefore, in principle both condensates need to be introduced.

In the low-energy regime, where nonperturbative effects dominate, effective models become indispensable tools for describing strongly interacting matter. Chiral Perturbation Theory (χ PT) stands out as a frequently employed effective framework, significantly contributing to the understanding of the vacuum structure of QCD and the properties of axions at low temperatures [74–79]. χ PT demonstrates notable

advantages in low-energy scenarios; for instance, its prediction of topological susceptibility at zero temperature aligns well with lattice QCD findings [80–82]. However, its applicability diminishes at high temperatures and/or large densities, as it lacks information about QCD phase transitions. Hence, there is a need for a QCD-like model capable of accommodating axions and capturing the QCD phase transition dynamics. One of the most popular is the Nambu-Jona-Lasinio (NJL) model, which describes the dynamics of fermions and their interactions through effective four-fermion interactions [59,69]. In the formulation of the model used in the present work it includes an instanton-induced interaction, which breaks the $U(1)_A$ symmetry, and it can describe both the spontaneous breaking of chiral symmetry and how quarks interact with axions.

The interaction of quark matter with axions has been already explored in [55,65–68,83,84], in the framework of the NJL model, where the effect of the chiral phase transition on the properties of the QCD axion was explored. Furthermore, the axion potential was studied at finite quark chemical potential, and the behavior of axion domain walls [13,85–89] (see also [90,91] for a pedagogical introduction to walls) in bulk quark matter was also investigated. It was found that the axion potential is very sensitive to the chiral phase transition, particularly when quark matter is near criticality, where the axion mass decreases and the self-coupling is enhanced. In this study, we aim to extend our previous work [83] considering the coupling of axions to diquarks, in order to take into account the effects of the presence of axions in a color-superconducting medium. Our model is based on a four-fermion effective interaction that contains a $U(1)_A$ -preserving term, that can be interpreted as an effective way to describe one-gluon exchange, as well as a $U(1)_A$ -breaking term, describing the instanton-mediated effective interaction. The relative strength of the two terms is regulated by a dimensionless, free parameter of the model, ζ , while the overall strength of the effective coupling, G_D , is chosen in order to reproduce a given value of the superconductive gap when ζ is varied. A previous study of the coupling of the axion to a color-supreconductive phase, based on chiral effective theories, can be found in [92].

Our main results are related to the study of the full topological susceptibility, $\chi = \partial^2 \Omega / \partial \theta^2$, in the color-superconductive phase. Here, Ω denotes the full thermodynamic potential of superconductive quark matter, while the derivative is understood at $\theta = 0$. We derive, within the model at hand, an exact analytical relation between χ and the physical value of the superconductive gap. χ is related to the axion mass, m_a , and decay constant, f_a , via $\chi = m_a^2 f_a^2$; therefore the knowledge of χ allows us to extract an explicit, analytical formula for m_a in the 2SC phase. Moreover, we compute the full axion potential, and extract from it the low-energy parameters of this potential: besides

m_a , we compute the axion self-coupling, λ . Within this work, we limit ourselves to a one-loop approximation (usually called the mean field approximation), leaving the study of the role of quantum fluctuations to future works.

The plan of the article is as follows. In Sec. II we describe the model we adopt in our work. In Sec. III we present our results regarding the superconductive gap at finite θ as well as the axion potential in the two-flavor superconductive phase. Finally, in Sec. IV we draw our conclusions and discuss possible future works. We use natural units $\hbar = c = k_B = 1$ throughout this paper.

II. THE MODEL

In this section, we present in some detail the model we use in our work. We firstly present the Lagrangian density, describing how we couple the axion to quarks in the superconductive phase of QCD. Next we turn to write the thermodynamic potential, computed at one loop. We then show the shape of this potential in the gaps space, discussing the location of its minima: this discussion is useful to understand the results we show in the next section. Finally, we present an approximated solution to the gap equation, valid for small $\theta = a/f_a$, that allows us to qualitatively understand the behavior of the superconductive gap versus θ .

A. Lagrangian density

To begin with, we consider the Lagrangian density

$$\begin{aligned} \mathcal{L}_{\text{int}} = & g_1 (q^T C i \gamma_5 \epsilon \epsilon q) (\bar{q} i \gamma_5 C \epsilon \epsilon \bar{q}^T) \\ & + g_2 (q^T C \epsilon \epsilon q) (\bar{q} C \epsilon \epsilon \bar{q}^T). \end{aligned} \quad (1)$$

This has been used in many works on the superconductive phases of QCD; see for example [63,64]. In those references, it is assumed that $g_1 = g_2$, so the $U(1)_A$ symmetry is preserved at the Lagrangian level. In this work, we assume $g_1 \neq g_2$ from the very beginning, in order to break the $U(1)_A$ symmetry at the level of the Lagrangian mimicking the instanton-mediated interaction. In the Lagrangian density (1) we used $C = -i\gamma_2\gamma_0$, satisfying $C^2 = C^\dagger C = -1$. Moreover, we adopted a condensed notation that suppresses the color and flavor indices carried by the fields and the antisymmetric symbols in every bilinear. For example,

$$q^T C i \gamma_5 \epsilon \epsilon q = q_{ai}^T C i \gamma_5 \epsilon_{\alpha\beta 3} \epsilon_{ij 3} q_{\beta j}, \quad (2)$$

here α, β denote color indices, while i, j stand for flavor indices.

Starting from (1), we isolate a term that is invariant under $U(1)_A$ and a term that explicitly breaks this symmetry. This can be easily achieved by adding and subtracting the terms $g_2 (q^T C i \gamma_5 \epsilon \epsilon q) (\bar{q} i \gamma_5 C \epsilon \epsilon \bar{q}^T)$ and $g_1 (q^T C \epsilon \epsilon q) (\bar{q} C \epsilon \epsilon \bar{q}^T)$; we then get

$$\begin{aligned} \mathcal{L}_{\text{int}} = & \frac{(g_1 + g_2)}{2} [(q^T C i \gamma_5 \epsilon \epsilon q) (\bar{q} i \gamma_5 C \epsilon \epsilon \bar{q}^T) \\ & + (q^T C \epsilon \epsilon q) (\bar{q} C \epsilon \epsilon \bar{q}^T)] \\ & + \frac{(g_1 - g_2)}{2} [(q^T C i \gamma_5 \epsilon \epsilon q) (\bar{q} i \gamma_5 C \epsilon \epsilon \bar{q}^T) \\ & - (q^T C \epsilon \epsilon q) (\bar{q} C \epsilon \epsilon \bar{q}^T)]. \end{aligned} \quad (3)$$

The first line in the above Lagrangian density is now $U(1)_A$ preserving, so we confined the breaking of $U(1)_A$ to the second line of (3). Writing $q = (\mathcal{P}_L + \mathcal{P}_R)q$, where

$$\mathcal{P}_R = \frac{1 + \gamma_5}{2}, \quad \mathcal{P}_L = \frac{1 - \gamma_5}{2}, \quad (4)$$

we can easily rewrite the second line of (3) as

$$\begin{aligned} & (g_1 - g_2) [(q^T C i \gamma_5 \mathcal{P}_L \epsilon \epsilon q) (\bar{q} i \gamma_5 \mathcal{P}_L C \epsilon \epsilon \bar{q}^T) \\ & + (q^T C i \gamma_5 \mathcal{P}_R \epsilon \epsilon q) (\bar{q} i \gamma_5 \mathcal{P}_R C \epsilon \epsilon \bar{q}^T)], \end{aligned} \quad (5)$$

where we used $\gamma_5 \mathcal{P}_L q = -\mathcal{P}_L q = -q_L$ and $\gamma_5 \mathcal{P}_R q = \mathcal{P}_R q = q_R$. Finally, defining $G_D = (g_1 + g_2)/2$ and $\zeta G_D = (g_1 - g_2)$, we can rewrite the interaction (1) as

$$\begin{aligned} \mathcal{L}_{\text{int}} = & G_D [(q^T C i \gamma_5 \epsilon \epsilon q) (\bar{q} i \gamma_5 C \epsilon \epsilon \bar{q}^T) + (q^T C \epsilon \epsilon q) (\bar{q} C \epsilon \epsilon \bar{q}^T)] \\ & + \zeta G_D [(q^T C i \gamma_5 \mathcal{P}_L \epsilon \epsilon q) (\bar{q} i \gamma_5 \mathcal{P}_L C \epsilon \epsilon \bar{q}^T) \\ & + (q^T C i \gamma_5 \mathcal{P}_R \epsilon \epsilon q) (\bar{q} i \gamma_5 \mathcal{P}_R C \epsilon \epsilon \bar{q}^T)]. \end{aligned} \quad (6)$$

The second line in (6) breaks $U(1)_A$: we consider it as an effective way to model the quark-quark interaction arising from the one-instanton exchange.

In order to couple the axions to the quarks, we note that the former can only couple to the $U(1)_A$ -breaking term in Eq. (6) (in fact, the QCD axion couples to instantonlike gluon configurations). In agreement with what has been done for the coupling to quarks in the vacuum [83], we write this coupling as

$$\begin{aligned} \mathcal{L}_{\text{int}} = & G_D [(q^T C i \gamma_5 \epsilon \epsilon q) (\bar{q} i \gamma_5 C \epsilon \epsilon \bar{q}^T) + (q^T C \epsilon \epsilon q) (\bar{q} C \epsilon \epsilon \bar{q}^T)] \\ & + \zeta G_D [e^{i\frac{a}{f_a}} (q^T C i \gamma_5 \mathcal{P}_L \epsilon \epsilon q) (\bar{q} i \gamma_5 \mathcal{P}_L C \epsilon \epsilon \bar{q}^T) \\ & + e^{-i\frac{a}{f_a}} (q^T C i \gamma_5 \mathcal{P}_R \epsilon \epsilon q) (\bar{q} i \gamma_5 \mathcal{P}_R C \epsilon \epsilon \bar{q}^T)]. \end{aligned} \quad (7)$$

The Lagrangian density (7) specifies the interaction we adopt in our model. As emphasized above, the first line in the right-hand side of (7) preserves the $U(1)_A$ symmetry, representing an effective way of writing the attractive channel of the quark-quark interaction arising from one-gluon exchange. The axial symmetry instead is broken by the terms in the second line [93,94]. We note that in [64], authors included both terms in the first line of (7); however, they usually neglect the second addendum in the first line of (7), since in the mean field, it gives rise to a pseudoscalar condensate that is usually neglected: as a matter of fact the

instanton-induced interaction, namely the second line of (7), favors condensation in the scalar channel when $a = 0$ (we explicitly verified this statement within our model; see below). However, when $a \neq 0$ condensation can happen in the pseudoscalar channel as well; therefore we need to consider the whole interaction (7).

In this work, we treat the interaction (7) within the mean-field approximation. In order to implement this, we introduce the condensates

$$\langle q^T C i \gamma_5 \mathcal{P}_L \varepsilon \varepsilon q \rangle = -h_L, \quad (8)$$

$$\langle \bar{q} i \gamma_5 \mathcal{P}_L C \varepsilon \varepsilon \bar{q}^T \rangle = h_R^*, \quad (9)$$

$$\langle q^T C i \gamma_5 \mathcal{P}_R \varepsilon \varepsilon q \rangle = h_R, \quad (10)$$

$$\langle \bar{q} i \gamma_5 \mathcal{P}_R C \varepsilon \varepsilon \bar{q}^T \rangle = -h_L^*, \quad (11)$$

as well as their combinations

$$\langle q^T C i \gamma_5 \varepsilon \varepsilon q \rangle = h_R - h_L, \quad (12)$$

$$\langle \bar{q} i \gamma_5 C \varepsilon \varepsilon \bar{q}^T \rangle = h_R^* - h_L^*. \quad (13)$$

Using these, as well as the assumptions $h_L = h_L^*$, $h_R = h_R^*$, we get, within the mean-field approximation,

$$\begin{aligned} \mathcal{L}_{\text{int}} = & G_D \varepsilon \varepsilon (h_R - h_L) [\langle \bar{q} i \gamma_5 C \varepsilon \varepsilon \bar{q}^T \rangle + \langle q^T C i \gamma_5 \varepsilon \varepsilon q \rangle] - G_D (h_R - h_L)^2 \\ & - G_D \varepsilon \varepsilon [(h_R + h_L) \langle \bar{q} i C \varepsilon \varepsilon \bar{q}^T \rangle - (h_R + h_L) \langle q^T C \varepsilon \varepsilon q \rangle] - G_D (h_R + h_L)^2 \\ & + \zeta G_D \varepsilon \varepsilon e^{i\frac{\pi}{f_a}} [-h_L \langle \bar{q} i \gamma_5 \mathcal{P}_L C \varepsilon \varepsilon \bar{q}^T \rangle + h_R \langle q^T C i \gamma_5 \mathcal{P}_L \varepsilon \varepsilon q \rangle] + \zeta G_D e^{i\frac{\pi}{f_a}} h_L h_R \\ & + \zeta G_D \varepsilon \varepsilon e^{-i\frac{\pi}{f_a}} [h_R \langle \bar{q} i \gamma_5 \mathcal{P}_R C \varepsilon \varepsilon \bar{q}^T \rangle - h_L \langle q^T C i \gamma_5 \mathcal{P}_R \varepsilon \varepsilon q \rangle] + \zeta G_D e^{-i\frac{\pi}{f_a}} h_L h_R. \end{aligned} \quad (14)$$

Note that $\mathcal{L}_{\text{int}} = \mathcal{L}_{\text{int}}^\dagger$.

In order to simplify the notation we introduce the Nambu-Gorkov bispinors

$$\Psi = \begin{pmatrix} q \\ C \bar{q}^T \end{pmatrix}, \quad \bar{\Psi} = (\bar{q}, q^T C). \quad (15)$$

In terms of these, we then can rewrite the interaction Lagrangian density as

$$\mathcal{L}_{\text{int}} = \mathcal{V} + \bar{\Psi} \Delta \Psi, \quad (16)$$

where

$$\mathcal{V} = -2G_D (h_R^2 + h_L^2) + 2\zeta G_D h_L h_R \cos\left(\frac{a}{f_a}\right), \quad (17)$$

and

$$\Delta = \begin{pmatrix} 0 & \Phi^- \\ \Phi^+ & 0 \end{pmatrix}, \quad (18)$$

with

$$\begin{aligned} \Phi^- = & G_D [2h_R \mathcal{P}_L - 2h_L \mathcal{P}_R - e^{ia/f_a} h_L \zeta \mathcal{P}_L \\ & + e^{-ia/f_a} h_R \zeta \mathcal{P}_R] i \gamma_5 \varepsilon_{ij} \varepsilon_{\alpha\beta 3} \end{aligned} \quad (19)$$

$$\begin{aligned} \Phi^+ = & G_D [2h_R \mathcal{P}_R - 2h_L \mathcal{P}_L + e^{ia/f_a} h_R \zeta \mathcal{P}_L \\ & - e^{-ia/f_a} h_L \zeta \mathcal{P}_R] i \gamma_5 \varepsilon_{ij} \varepsilon_{\alpha\beta 3}. \end{aligned} \quad (20)$$

In the above equations, the first two terms arise from the one-gluon exchange interaction, while those proportional to ζ arise from the one-instanton exchange. The matrix Δ has a similar structure to that of [63]: indeed, it satisfies $\Phi^+ = \gamma_0 (\Phi^-)^\dagger \gamma_0$.

To the interaction (16) we need to add the kinetic term of quarks at finite chemical potential μ . This contribution is well known [63,64] and leads to the full Lagrangian, that in momentum space reads as

$$\mathcal{L} = \mathcal{V} + \bar{\Psi} S^{-1} \Psi. \quad (21)$$

Here, the inverse quark propagator is given by

$$S^{-1}(p) = \begin{pmatrix} (p + \mu \gamma_0) \mathbf{1}_C \mathbf{1}_F & \Phi^- \\ \Phi^+ & (p - \mu \gamma_0) \mathbf{1}_C \mathbf{1}_F \end{pmatrix}, \quad (22)$$

where $\mathbf{1}_C$ and $\mathbf{1}_F$ correspond to the identities in color and flavor spaces respectively. We note that these matrices have dimension $4 \times 3 \times 2 \times 2 = 48$, due to Dirac, color, flavor, and Gorkov indices, respectively.

B. Thermodynamic potential

The thermodynamic potential is obtained via the standard integration over the fermion fields in the partition function [63,64], which leads at

$$\Omega = -\mathcal{V} + \Omega_{\text{1-loop}}, \quad (23)$$

where \mathcal{V} denotes the mean-field contribution (17), and $\Omega_{1\text{-loop}}$ corresponds to the 1-loop contribution of the quarks, namely

$$\Omega_{1\text{-loop}} = -T \sum_n \int \frac{d^3 p}{(2\pi)^3} \frac{1}{2} \text{Tr} \log (\beta S^{-1}(i\omega_n, \vec{p})). \quad (24)$$

In getting Eq. (24) we performed the functional integral over fermions at fixed a : in fact, in this work the axion field is treated as a classical background. Consequently, the thermodynamic potential is a function of a , and physical quantities have to be computed at a given value of a . Moreover, we used the imaginary time formalism of finite temperature field theory, and $\omega_n = (2n + 1)\pi T$ are the relevant fermionic Matsubara frequencies. The overall 1/2 in (24) takes into account the artificial doubling of degrees of freedom introduced by shifting to the Nambu-Gorkov bispinors. Finally, the trace is understood in Nambu-Gorkov, Dirac, color and flavor spaces.

In order to evaluate the sum over ω_n in Eq. (24), we follow the well-known strategy of computing the eigenvalues of the matrix [63,64]

$$\mathcal{T} = \begin{pmatrix} (-\gamma_0 \vec{p} \cdot \vec{\gamma} + \mu) \mathbf{1}_C \mathbf{1}_F & \gamma_0 \Phi^- \\ \gamma_0 \Phi^+ & (-\gamma_0 \vec{p} \cdot \vec{\gamma} - \mu) \mathbf{1}_C \mathbf{1}_F \end{pmatrix}. \quad (25)$$

These are given by

$$\varepsilon_{1,\pm} = \pm |p - \mu|, \quad (26)$$

$$\varepsilon_{2,\pm} = \pm |p + \mu|, \quad (27)$$

$$\varepsilon_{3,\pm} = \pm \sqrt{(p - \mu)^2 + \Delta_3^2}, \quad (28)$$

$$\varepsilon_{4,\pm} = \pm \sqrt{(p + \mu)^2 + \Delta_3^2}, \quad (29)$$

$$\varepsilon_{5,\pm} = \pm \sqrt{(p - \mu)^2 + \Delta_5^2}, \quad (30)$$

$$\varepsilon_{6,\pm} = \pm \sqrt{(p + \mu)^2 + \Delta_5^2}, \quad (31)$$

where $p \equiv |\mathbf{p}|$ denotes the magnitude of the 3-momentum \mathbf{p} ; each of the eigenvalues above has a multiplicity equal to 4. The eigenvalues (26) and (27) correspond to those of the blue quarks, which do not participate to the pairing and remain ungapped. Moreover, we put

$$\Delta_3^2 = \zeta^2 G_D^2 h_L^2 + 4G_D^2 h_R^2 - 4\zeta G_D^2 h_L h_R \cos(a/fa), \quad (32)$$

$$\Delta_5^2 = \zeta^2 G_D^2 h_R^2 + 4G_D^2 h_L^2 - 4\zeta G_D^2 h_L h_R \cos(a/fa), \quad (33)$$

that represent the (squared) gaps in the quark spectrum.

Putting $\varepsilon_k(\vec{p}) = \varepsilon_{k,+}(\vec{p})$, $k = 1, \dots, 6$, we use $\text{In det } \beta S^{-1} = \text{Tr} \text{In } \beta S^{-1}$ and write

$$\text{In det } \beta S_L^{-1}(i\omega_n, \vec{p}) = 4 \sum_{k=1}^6 \ln \left(\frac{\omega_n^2 + \varepsilon_k(\vec{p})^2}{T^2} \right), \quad (34)$$

where we made explicit the degeneracy, equal to 4, of the eigenvalues and matched the ones with opposite signs. Now the Matsubara sum can be easily evaluated, since

$$T \sum_n \ln \left(\frac{\omega_n^2 + \varepsilon_k(\vec{p})^2}{T^2} \right) = |\varepsilon_k(\vec{p})| + 2T \ln(1 + e^{-|\varepsilon_k(\vec{p})|/T}), \quad (35)$$

so the 1-loop contribution finally results in

$$\Omega_{1\text{-loop}}^L = -2 \sum_{k=1}^6 \int \frac{d^3 p}{(2\pi)^3} [\varepsilon_k(\vec{p}) + 2T \ln(1 + e^{-\varepsilon_k(\vec{p})/T})], \quad (36)$$

where we took into account that according to our definitions the ε_k are always positive. Therefore, the thermodynamic potential is given by

$$\Omega = 2G_D(h_R^2 + h_L^2) - 2\zeta G_D h_L h_R \cos\left(\frac{a}{fa}\right) - 2 \sum_{k=1}^6 \int \frac{d^3 p}{(2\pi)^3} [\varepsilon_k(\vec{p}) + 2T \ln(1 + e^{-\varepsilon_k(\vec{p})/T})]. \quad (37)$$

The first addendum in the right-hand side of (36) corresponds to the $T = 0$ contribution to the thermodynamic potential, which is divergent in the ultraviolet. In order to regulate this divergence, we introduce a sharp 3D momentum cutoff, Λ , and rewrite that term as

$$\int \frac{d^3 p}{(2\pi)^3} \varepsilon_k(p) = \frac{4\pi}{8\pi^3} \int_0^\Lambda p^2 dp \varepsilon_k(p). \quad (38)$$

The cutoff roughly represents the momentum scale above which the contact interaction used in the present work should be replaced by a nonlocal term directly borrowed from QCD. We treat Λ as a free parameter of the model, and from previous studies based on the NJL model, we assume $\Lambda = O(1 \text{ GeV})$. We also notice that we inserted no cutoff in the thermal part because it is finite; however in previous studies, based on NJL models at zero baryon density, this cutoff was introduced, and it was shown to mildly affect thermodynamic quantities, particularly near the critical temperature for chiral-symmetry restoration [95–97]. In fact, the cut of high momenta in the loop could be interpreted as a very rough implementation of a momentum-dependent mass

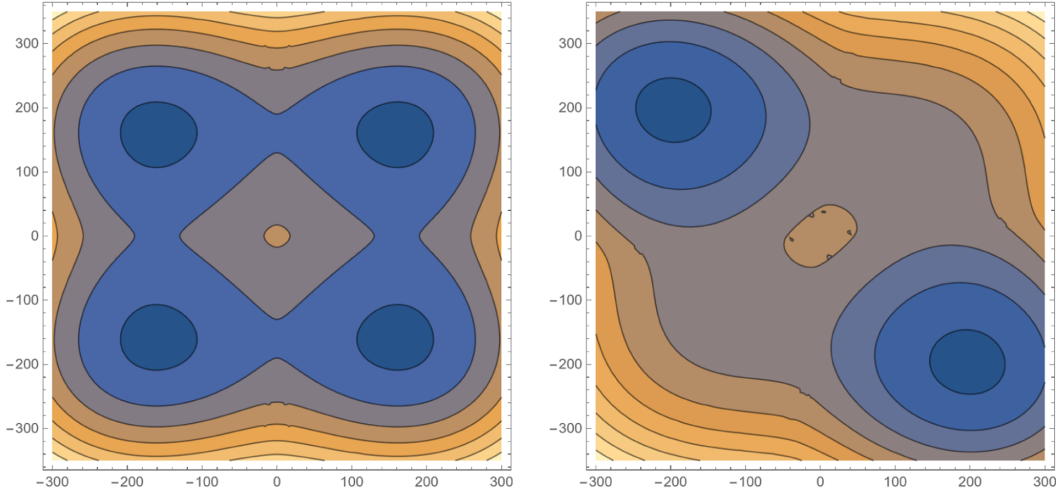


FIG. 1. Thermodynamic potential at $T = 0$, computed for $\theta \equiv a/f_a = 0$, and for $\zeta = 0$ (left panel) and for $\zeta = 0.2$ (right panel). In the plots, x and y axes denote Δ_L and Δ_R respectively (measured in MeV).

function. The analysis of this occurrence, although very interesting, is beyond the scope of the present study; therefore we leave it to a future work.

We notice that although in (36) we sum over the six positive eigenvalues of \mathcal{T} , the ones corresponding to the blue quarks, which do not participate in the pairing, do not contribute to the value of the condensates.

It is useful to stress that both \mathcal{V} and the quark spectrum are invariant under the set of transformations $h_L \leftrightarrow h_R$ and $h_L \leftrightarrow -h_R$; moreover, if $\zeta = 0$ then Ω depends on h_L^2 and h_R^2 only: as a consequence, in this limit we expect Ω to develop a set of four degenerate minima along the lines $h_L = \pm h_R$. This degeneracy is removed by $\zeta \neq 0$. This picture is confirmed by the direct evaluation of Ω ; see Fig. 1 in the next section.

C. Thermodynamic potential at finite $\theta = a/f_a$:

The lines $h_L = \pm h_R$

In this subsection, we analyze the shape of Ω in the (h_L, h_R) plane: this is preparatory to the results on the gap that we present in the next section. In Fig. 1 we plot the thermodynamic potential at $T = 0$, computed for $\theta \equiv a/f_a = 0$, and for $\zeta = 0$ (left panel) and for $\zeta = 0.2$ (right panel). In the plots, x and y axes denote Δ_L and Δ_R respectively (measured in MeV), which are defined as

$$\Delta_L = 2G_D h_L, \quad \Delta_R = 2G_D h_R. \quad (39)$$

It is more convenient to use $\Delta_{L,R}$ instead of $h_{L,R}$ since the former correspond to the gaps in the quark spectrum when $\zeta = 0$. From these, we can introduce the following scalar and pseudoscalar combinations as

$$\Delta_S = \Delta_R - \Delta_L, \quad \Delta_{PS} = \Delta_R + \Delta_L. \quad (40)$$

We notice in Fig. 1 that for $\zeta = 0$, namely when we only consider the one-gluon-exchange interaction, there are four loci of degenerate minima. Two of these correspond to $\Delta_L = \Delta_R$ and therefore to finite pseudoscalar condensate and vanishing scalar condensate whereas the other two correspond to $\Delta_L = -\Delta_R$ and consequently to finite scalar condensate and vanishing pseudoscalar condensate.

On the other hand, when the instanton-induced interaction is switched on ($\zeta \neq 0$) this degeneracy is removed, and the condensation in the scalar channel $\Delta_L = -\Delta_R$ is favored.

In Fig. 2 we plot the thermodynamic potential at $T = 0$, computed for $\zeta = 0.2$, and several values of $\theta \equiv a/f_a$. In each plot, x and y axes denote Δ_L and Δ_R respectively (measured in MeV). In the figure, the top left plot corresponds to $\theta = 0$, top right to $\theta = \pi/2 - \varepsilon$, center left to $\theta = \pi/2$, center right to $\theta = \pi/2 + \varepsilon$, with $\varepsilon = 0.25$, bottom left to $\theta = 3\pi/2$, and finally bottom right to $\theta = 2\pi$. For all the cases shown in the figure, the minima of Ω sit on the lines $\Delta_L = \pm \Delta_R$: this is the obvious consequence of the fact that Ω is invariant under the transformations $h_L \leftrightarrow \pm h_R$. For a/f_a in the range $[0, \pi/2)$, the global minima correspond to $\Delta_L = -\Delta_R$; hence, in this range of a/f_a only the scalar condensate exists. The minima become less shallow as a/f_a is increased: indeed, for a/f_a in the range $(\pi/2, 3\pi/2)$ the global minima are located along the line $\Delta_L = \Delta_R$, implying a phase transition from the scalar to the pseudoscalar condensate. Finally, increasing a/f_a up to 2π the location of the minima changes again in another phase transition from the pseudoscalar to the scalar condensate. Along the lines $\Delta_L = \pm \Delta_R$ we have $\Delta_3 = \Delta_5$ for any a and ζ : hence, there is only one gap in the quark spectrum; see (32) and (33).

We notice that the results on the minima of Ω discussed above stand for $\zeta > 0$: we checked that for $\zeta < 0$ the role of

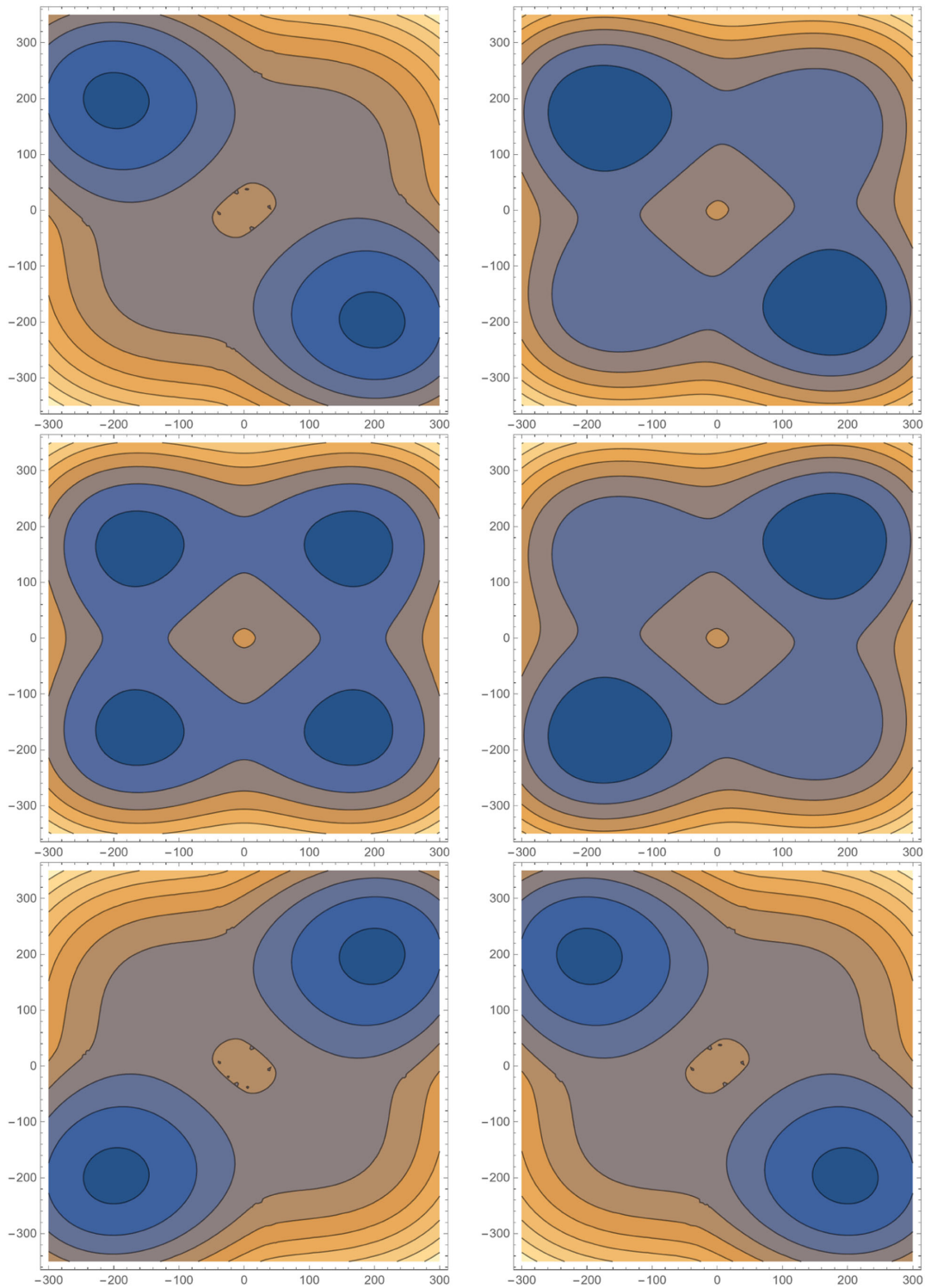


FIG. 2. Thermodynamic potential at $T = 0$, computed for $\zeta = 0.2$, and several values of $\theta \equiv a/f_a$. In each plot, x and y axes denote Δ_L and Δ_R respectively (measured in MeV). Top left plot corresponds to $\theta = 0$, top right to $\theta = \pi/2 - \epsilon$, center left to $\theta = \pi/2$, center right to $\theta = \pi/2 + \epsilon$, with $\epsilon = 0.25$, bottom left to $\theta = \pi$, and finally bottom right to $\theta = 2\pi$.

the scalar and the pseudoscalar condensates invert; besides this, there is no major difference between the system with positive and negative ζ . Consequently, from now on we limit ourselves to show results for $\zeta > 0$ only.

Before going ahead, we determine the allowed values of ζ that lead to the nontrivial solution of the gap equation. To this end, it is enough to limit ourselves to the gap equation at $T = 0$ and small θ . Imposing the stationarity condition of

Ω with respect to h_L , namely $\partial\Omega/\partial h_L = 0$ with Ω given by Eq. (37), and then applying this condition along the line $h_L = -h_R$, which is the one along which Ω develops minima for small θ as discussed above, gives

$$2 + \zeta \cos(a/f_a) = \frac{G_D}{2\pi^2} \int_0^\Lambda p^2 dp \left(\frac{A(a, \zeta)}{\sqrt{(p-\mu)^2 + G_D^2 h_L^2 A(a, \zeta)}} + \mu \rightarrow -\mu \right), \quad (41)$$

where we removed the trivial solution $h_L = 0$, and we defined

$$A(a, \zeta) = 4 + 4\zeta \cos(a/f_a) + \zeta^2. \quad (42)$$

The above equation shows that the condition $\zeta < 2$ must be satisfied in order to have a nontrivial solution of the gap equation. In fact, the right-hand side of (41) is always positive, and so the left-hand side must be positive as well: this can be obtained for all values of a if and only if $\zeta < 2$. For $\zeta \geq 2$ there is a range of a in which the gap equation has only the trivial solution $h_L = 0$: hence, in what follows we limit ourselves to $\zeta < 2$.

III. RESULTS

A. Gaps versus a/f_a

In this subsection, we present our results for the gap parameters. For $\Delta_L = \pm\Delta_R$, which correspond to the directions along which the minima develop at finite a , we get from Eqs. (32) and (33) that $\Delta_3 = \Delta_5$. Therefore we limit ourselves to show results for Δ_3 only. We fix $\mu = 400$ MeV and $\Lambda = 1$ GeV as representative values of the quark chemical potential and the UV cutoff. For each ζ , we fix G_D in order to have a desired value of Δ_L at $a = 0$.

In Fig. 3 we plot Δ_L and Δ_R versus a/f_a at $T = 0$ and $\mu = 400$ MeV; we consider several values of ζ , while G_D is fixed for each ζ so that $\Delta_L = 50$ MeV at $a = 0$. We firstly focus on the results for $\zeta = 0.2, 0.5$ and 1 . For these values of ζ , we notice that for a/f_a in the range $(0, \pi/2)$, $\Delta_R = -\Delta_L$; hence only the scalar condensate forms. On the other hand, for a/f_a in the range $(\pi/2, 3\pi/2)$, $\Delta_R = \Delta_L$. In this case, only the pseudoscalar condensate forms. Finally, for a/f_a in the range $(3\pi/2, 2\pi)$ we find again $\Delta_R = -\Delta_L$; hence there is a phase transition from the pseudoscalar to the scalar condensate. We also notice that for $\zeta = 1.6$ and $\zeta = 1.75$ the magnitude of Δ_L increases with a for a/f_a in the range $(0, \pi/2)$.

The results in Fig. 3 show several interesting features. In fact, as we already pointed out, there is a noticeable qualitative difference in dependency of Δ_L when comparing the three lowest values of ζ with the higher ones. In particular, Δ_L decreases close to $a/f_a = 0$ for $\zeta = 0.2, \zeta = 0.5$ and $\zeta = 1.0$, and it exhibits a local minimum at $a/f_a = \pi/2$ and $3\pi/2$. Furthermore one can observe a discontinuity in its derivative at the aforementioned minimum points, for the three lowest values of ζ , where the derivative changes sign. In contrast, for the highest value of ζ , i.e. $\zeta = 1.75$, we observe that Δ_L increases in the proximity of $a/f_a = 0$. This suggests the presence of a critical value of ζ where the change from positive to negative curvature at $a/f_a = 0$ occurs. This is indeed the case, and its value is derived in Eq. (49). The change in the behavior of Δ_L can already be observed for an intermediate value of ζ , i.e., $\zeta = 1.6$. In this case one can see that the curve in the proximity of a/f_a is still increasing but almost flat, signaling the proximity to the aforementioned critical point. Furthermore we continue to observe local minima and cusps at $a/f_a = \pi/2$ and $3\pi/2$. This signals the emergence of two local maxima in the ranges $a/f_a = [0, \pi/2]$ and $a/f_a = [\pi/2, \pi]$ (and the corresponding ones in the ranges $a/f_a = [0, \pi/2]$ and $a/f_a = [\pi/2, \pi]$

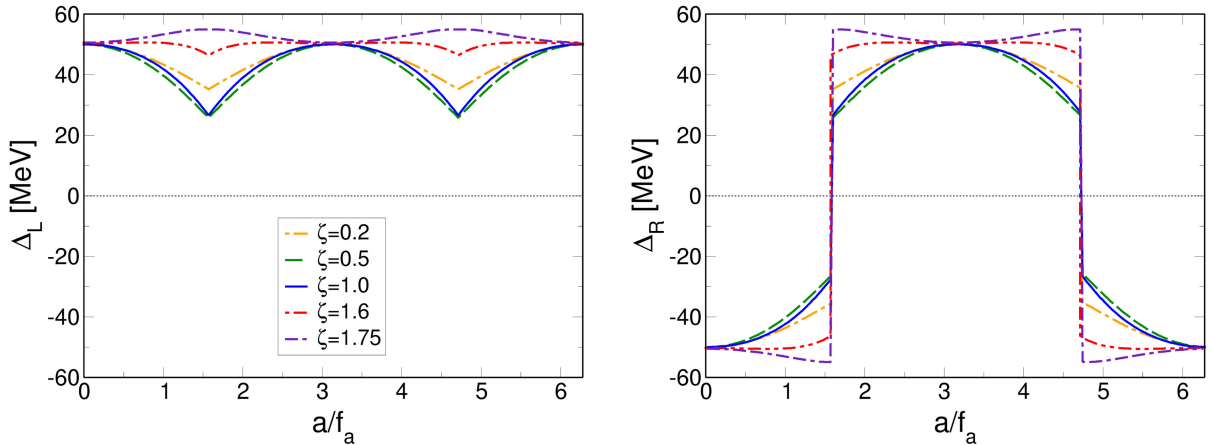


FIG. 3. Gaps Δ_L and Δ_R at $T = 0$ and $\mu = 400$ MeV, versus a/f_a , and for several values of ζ . G_D is fixed in order to have $\Delta_L = 50$ MeV for $a = 0$ at $\mu = 400$ MeV.

considering the periodicity of π). Although less evident, the same behavior is also present for $\zeta = 1.75$. According to our line of reasoning then, we also conclude that $a/f_a = n\pi$ (n integer) turn from being local maxima in the case of lower values of ζ , to local minima for the higher ones. From our previous discussion on the transition between scalar and pseudoscalar condensates, the behavior of Δ_R , shown in the left panel of Fig. 3, can be straightforwardly understood from the corresponding one of Δ_L .

The behavior of Δ_L near $a = 0$ can be semiquantitatively understood by the approximate solution of the gap equation (41), namely

$$\Delta_L = \frac{4\delta}{\sqrt{A(a, \zeta)}} \exp\left(-\frac{\pi^2}{\mu^2 G_D \Theta(a, \zeta)}\right), \quad (43)$$

where A is given by Eq. (42) and

$$\Theta(a, \zeta) = \frac{A(a, \zeta)}{2 + \zeta \cos(a/f_a)}. \quad (44)$$

The approximated solution (43) can be obtained within the High Density Effective Theory (HDET) of QCD (see [98] and references therein), as well as Appendix A; it has the standard form of the Bardeen-Cooper-Schrieffer (BCS) gap in the theory of superconductivity [99,100]: in fact, μ^2 is proportional to the density of states of the pairing quarks at the Fermi surface, and δ in (43) plays the role of the Debye frequency, ω_D , of the BCS theory, which cuts high momentum modes out of the pairing. The solution (43) is strictly valid only in the weak coupling; hence it cannot quantitatively reproduce the results in Fig. 3; however, it is still helpful to grasp the behavior of Δ_L near $a = 0$. In fact, from (43) we notice that for a fixed value of ζ , the coupling of the superconductive quarks to the axion field effectively affects the pairing in two ways. Firstly, it changes the width of the shell around the Fermi surface that contributes to the pairing, namely

$$\frac{2\delta}{\sqrt{A(0, \zeta)}} \rightarrow \frac{2\delta}{\sqrt{A(a, \zeta)}}. \quad (45)$$

Secondly, it effectively changes the chemical potential of the quarks, that is

$$\mu^2 \Theta(0, \zeta) \rightarrow \mu^2 \Theta(a, \zeta). \quad (46)$$

Both $A(a, \zeta)$ and $\Theta(a, \zeta)$ are decreasing functions of a at fixed ζ . Consequently, the response of Δ_L to the coupling with the axion has two competing effects: on the one hand, it leads to the opening of the shell around the Fermi surface, thus increasing the portion of phase space involved in the pairing; on the other hand, it effectively lowers the chemical potential of the paired quarks, implying the decrease of the volume of phase space

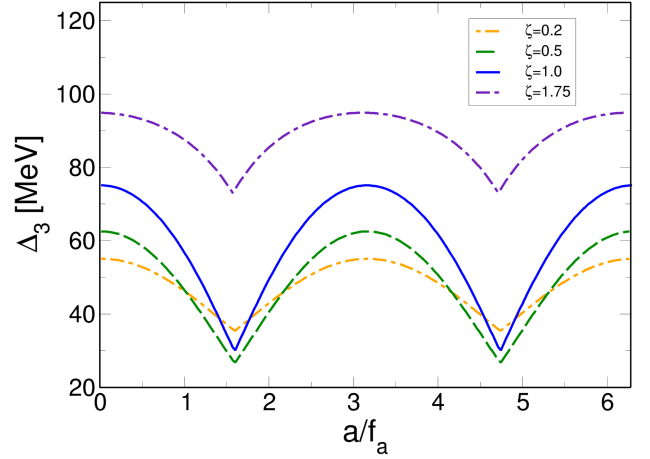


FIG. 4. Gap in the quark spectrum, Δ_3 , at $T = 0$ and $\mu = 400$ MeV, versus a/f_a , and for several values of ζ . G_D is fixed in order to have $\Delta_L = 50$ MeV for $a = 0$ at $\mu = 400$ MeV.

available for pairing. Which of the two effects wins depends, at a given G_D , on the value of ζ . This can be seen by inspecting the curvature of Δ_L for small $\theta = a/f_a$. To this end, it is enough to expand Eq. (43) near $\theta = 0$, getting

$$\Delta_L = \Delta_{L,0} \left(1 + \frac{\kappa}{2} \theta^2\right), \quad (47)$$

where $\Delta_{L,0}$ denotes the gap (43) at $\theta = 0$, and the curvature is

$$\kappa = \zeta \frac{\pi^2(\zeta - 2) + 2G_D\mu^2(2 + \zeta)}{G_D\mu^2(2 + \zeta)^4}. \quad (48)$$

The curvature is trivially zero for $\zeta = 0$, as well as for

$$\zeta = \zeta_{\text{crit}} = \frac{2(\pi^2 - G_D\mu^2)}{\pi^2 + G_D\mu^2}; \quad (49)$$

it is negative for ζ in the range $(0, \zeta_{\text{crit}})$, and positive otherwise. Hence, the response of Δ_L to θ around $\theta = 0$ depends on the specific value of ζ , and the turning point of ζ , namely ζ_{crit} , depends on the value of G_D .

The gap in the quark spectrum, along the global minima lines, is given by Δ_3 in (32). We show Δ_3 versus a/f_a in Fig. 4. We notice that Δ_3 is a periodic function of a/f_a , with a period equal to π , as expected from the results on Δ_L and Δ_R shown Fig. 3. We find that although the response of Δ_L and Δ_R on a/f_a depends on ζ , hence on the weight of the $U(1)_A$ -breaking interaction term, the qualitative behavior of Δ_3 does not depend on ζ .

B. Axion potential

One of the main results of our work is the computation of the axion potential, $V(a/f_a)$, in a superconductive phase of

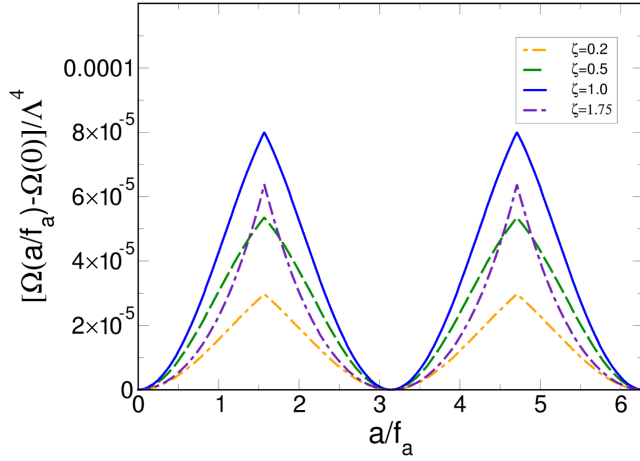


FIG. 5. Axion potential, $V(\theta) = \Omega(\theta) - \Omega(0)$ with $\theta = a/f_a$, versus a/f_a , computed at $T = 0$ and $\mu = 400$ MeV and for several values of ζ . The potential is measured in units of Λ^4 with $\Lambda = 1$ GeV. G_D is fixed to have $\Delta_L = 50$ MeV at $a = 0$.

QCD. In Fig. 5 we plot the $V(a/f_a) \equiv \Omega(a/f_a) - \Omega(a/f_a = 0)$ versus a/f_a , at $T = 0$ and $\mu = 400$ MeV. For each value of a/f_a , the potential has been computed at the global minimum in the (Δ_L, Δ_R) space. The behavior of V is in agreement with that of the quark spectrum shown in Fig. 4, particularly for what concerns the periodicity. We notice that $a = 0$ is a global minimum of $V(a/f_a)$ for the whole range of parameters studied here. Other degenerate minima are located at $a/f_a = n\pi/2$ with $n = \pm 1, \pm 2, \dots$

It is useful to stress the difference with respect to the axion potential computed in the presence of the chiral and the η condensate [83] at zero baryon density: indeed, in that case, the periodicity of $V(a/f_a)$ is equal to 2π , while in the case of superconductive matter, we find a periodicity equal to π . This can be understood easily. In fact, in the present case at $a = 0$ only the scalar condensate forms, then increasing the value of a the global minima become less shallow and at $a/f_a = \pi/2$ the thermodynamic potential develops four degenerate minima, see Fig. 2. Further increasing a/f_a in the range $(\pi/2, 3\pi/2)$ results in the rotation of the global minima of Ω and in the consequent formation of the pseudo-scalar condensate. The ground states at $a = 0$ and $a/f_a = \pi$ are degenerate, hence the periodicity of the potential, but the two adjacent minima correspond to two different condensation channels: in particular, the ground state at $a = 0$ is characterized by scalar condensation, while the minimum at $\theta = \pi/2$ corresponds to condensation in the pseudoscalar channel.

C. Topological susceptibility

In this section, we analyze the full topological susceptibility, χ , which measures the fluctuations of the topological charge and is defined as

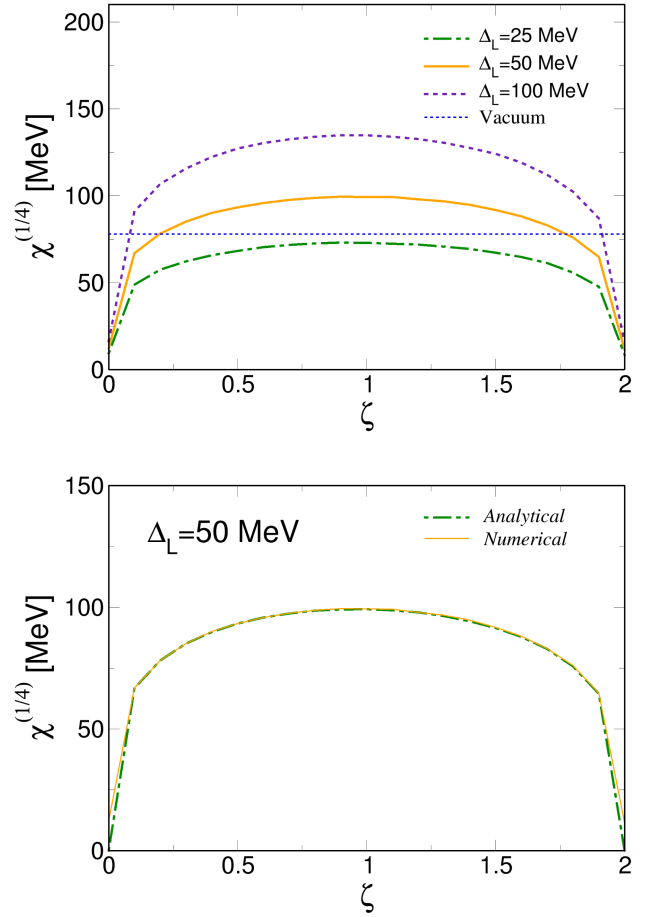


FIG. 6. Topological susceptibility, $\chi^{1/4}$, versus ζ , at $T = 0$ and for several values of Δ_L . We used $\mu = 400$ MeV, $\Lambda = 1000$ MeV. The value of Δ_L in the legend has been used to fix the value of G_D , so that for each line Δ_L is kept fixed while ζ is changed. The horizontal blue line corresponds to the reference value expected for the topological susceptibility in the vacuum; see, e.g., [65,80]. The analytical curve corresponds to Eq. (52) computed for $\Delta_L = 50$ MeV and $G_D\Lambda^2 = 4.69$.

$$\chi = \left. \frac{d^2\Omega}{d\theta^2} \right|_{\theta=0}, \quad \theta = \frac{a}{f_a}. \quad (50)$$

In the numerical calculation, we treat the above derivative as a total derivative, that in principle takes into account also the dependence of the condensates on θ at $\theta = 0$.

In Fig. 6 we plot the fourth root of χ versus ζ , at $T = 0$ and for several values of Δ_L . We used $\mu = 400$ MeV, $\Lambda = 1000$ MeV. The value of Δ_L in the legend has been used to fix the value of G_D , so that for each line Δ_L is kept fixed while ζ is changed. χ is an interesting quantity by itself, since it encodes information about the fluctuations of the topological charge in the dense and superconductive QCD medium. Moreover, it is directly related to the squared axion mass; see the next subsection. Previous studies performed within lattice QCD in the isospin-symmetric case, as well as within chiral perturbation theory

and NJL models, agree on the value $\chi^{1/4} \approx 78$ MeV at $T = 0$ and $\mu = 0$ [9,65,80,101], as well as with the Di Vecchia-Crewther-Leutwyler-Smilga-Veneziano formula [102–105], that for two flavors reads as

$$\chi = |\langle \bar{q}q \rangle| \frac{m_u m_d}{m_u + m_d}, \quad (51)$$

where $\langle \bar{q}q \rangle$ is the chiral condensate in the vacuum. χ then decreases at high T where the smooth crossover to the quark-gluon plasma phase takes place [9,65,80,101].

The results in Fig. 6 show that for a given value of ζ , the topological susceptibility increases with the strength of the coupling, as expected. Moreover, if the coupling is tuned in order to give a value of Δ_L , changing ζ within the range (0.5,1.5) does not substantially affect $\chi^{1/4}$. We also note that keeping ζ in the aforementioned range keeps $\chi^{1/4}$ in the superconductive phase in the same ballpark of the value it takes in the vacuum, unless we take a very large superconductive gap as in the case of $\Delta_L = 100$ MeV shown in Fig. 6.

Within our model we were able to obtain an analytical result for χ . In fact, taking into account that at the global minimum $\partial\Omega/\partial\Delta_L = \partial\Omega/\partial\Delta_R = 0$, and according to the results in Fig. 3 we have $\partial\Delta_L/\partial\theta = \partial\Delta_R/\partial\theta = 0$ at $\theta = 0$ [see also Eq. (47)], it is straightforward to prove that (see Appendix B)

$$\chi = \frac{\Delta_L^2}{2G_D} \zeta \frac{2 - \zeta}{2 + \zeta}, \quad (52)$$

where Δ_L corresponds to the solution of the gap equation at $\theta = 0$; Eq. (52) stands both at zero and at finite temperature. In the bottom panel of Fig. 6 we plot the fourth root of the topological susceptibility versus ζ , obtained by Eq. (52) using $\Delta_L = 50$ MeV and $G_D \Lambda^2 = 4.69$. The agreement between the analytical result and the numerical one is self-explanatory (we checked the agreement also for other values of the parameters).

D. Axion mass and self-coupling

The low-energy Lagrangian density of the axion field can be written as

$$\mathcal{L}_a = \frac{1}{2} \partial^\mu a \partial_\mu a - \frac{m_a^2}{2} a^2 - \frac{\lambda_a}{4!} a^4, \quad (53)$$

where the axion mass and the quartic coupling are defined in terms of the potential $V(\theta) = \Omega(\theta) - \Omega(0)$ as

$$m_a^2 = \frac{1}{f_a^2} \frac{d^2 \Omega}{d\theta^2} \Big|_{\theta=0}, \quad \lambda_a = \frac{1}{f_a^4} \frac{d^4 V(\theta)}{d\theta^4} \Big|_{\theta=0}, \quad (54)$$

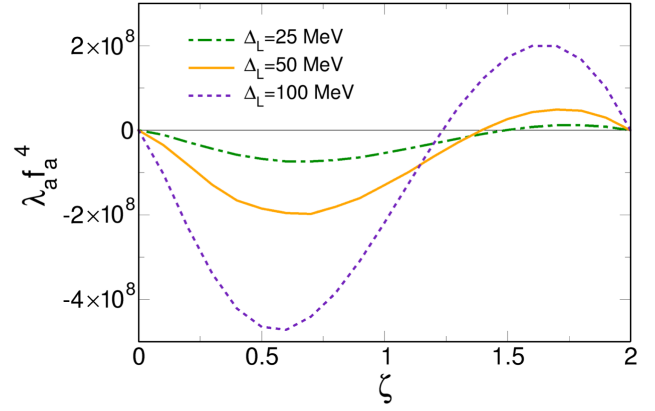


FIG. 7. Axion self-coupling, $\lambda_a f_a^4$, versus ζ for several values of Δ_L .

and $\theta = a/f_a$. Within our model, we can compute how the axion mass and coupling behave in the superconductive phase of QCD, as well as study their response to the phase transition to the normal phase.

From (B8) we get an analytical formula for the axion-squared mass in the color-superconductive phase, which is

$$m_a^2 = \frac{\Delta_L^2}{2G_D f_a^2} |\zeta| \frac{2 - |\zeta|}{2 + |\zeta|}, \quad (55)$$

where Δ_L corresponds to the solution of the gap equation. To our knowledge, Eq. (55) is a new result in the literature.

We have not been able to find an analytical expression for λ_a ; hence we computed it numerically. In Fig. 7 we plot the rescaled axion self-coupling, versus ζ , for several values of Δ_L . The parameters are the same as used in Fig. 6. For the sake of comparison, we note that studies based on the NJL model find $\lambda_a f_a^4 = -(55.64 \text{ MeV})^4$ at $T = \mu = 0$ [65]. We find that λ_a is negative in a range of ζ that partly depends on Δ_L , hence on the strength of the coupling. This sign of λ_a is in agreement with what was found within NJL models at zero as well as finite μ [65,83]. However, we find also a range of ζ where λ_a is positive. The value $\bar{\zeta}$ of $\zeta \neq 0$ such that $\lambda_a = 0$ depends on the strength of the coupling; however, comparing with the results shown in Fig. 3, we find that $\bar{\zeta}$ is in agreement with the value at which Δ_L and Δ_R invert their tendency to change as a/f_a is increased [see Eq. (49)].

E. Finite temperature

In this section, we briefly investigate the axion potential in dense superconductive quark matter at a small, albeit finite, temperature. Increasing the temperature we expect a critical value, depending on the chemical potential, for which a phase transition occurs from the color-superconducting phase to normal-quark matter. In particular, when the critical temperature T_c is reached, the gaps Δ_L and Δ_R

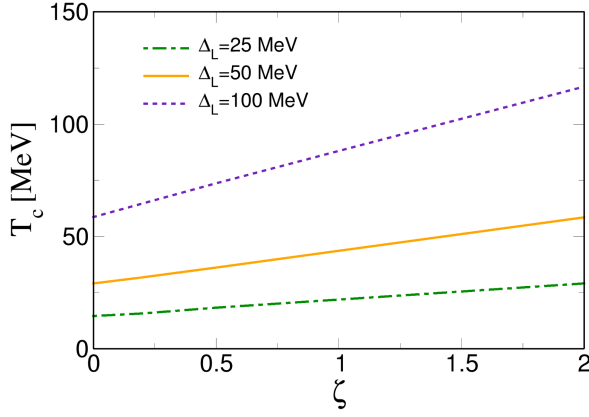


FIG. 8. Critical temperature, T_c , as a function of ζ , for different values of Δ_L . Calculations correspond to $a = 0$.

vanish, and a second-order phase transition occurs. We do not push this investigation too much, because we neglected quark masses in this work, that contribute to obtain nonzero values of χ and λ_a above the critical temperature: we limit ourselves to compute how T_c depends on ζ , as well as to show the behavior of χ and λ_a around T_c obtained within our model.

In Fig. 8 we plot T_c versus ζ for several values of Δ_L ; G_D is varied as a function of ζ , such that along each line the value of Δ_L at $T = 0$ is kept constant. We find that T_c increases linearly as a function of ζ ; moreover, T_c increases upon increasing Δ_L as expected. This is in agreement with the analytic result that can be found within the framework of the HDET,

$$T_c = \Delta_L^0 \frac{e^\gamma(2 + \zeta)}{2\pi}, \quad (56)$$

where Δ_L^0 is the value of the gap at vanishing temperature and $\gamma \approx 0.577$ is the Euler-Mascheroni constant. See Appendix C for a derivation of (56).

It is also interesting to check the behavior of $\chi^{1/4}$ and λ_a versus T near the transition to normal quark matter. In particular, we verified that Eq. (52) is also valid in the finite-temperature case (see Appendix B), and the temperature dependence enters only via Δ_L . In the upper panel of Fig. 9 we show the topological susceptibility, $\chi^{1/4}$ (upper panel) and axion self-coupling, $\lambda_a f_a^4$ (lower panel), versus T for $\zeta = 1$. We used $\mu = 400$ MeV and $\Delta_L = 25$ MeV. The trend we find is in agreement with Eq. (52), with a vanishing χ and λ_a in the normal phase. However, we remark that the vanishing of these two quantities in the normal phase is an artifact of our one-loop approximation to the thermodynamic potential, as well as neglecting the quark masses: including quark masses would lead to nonzero axion mass and self-coupling also in the normal phase, similarly to what happens in the high temperature/low density region of the QCD phase diagram [9,65,83].

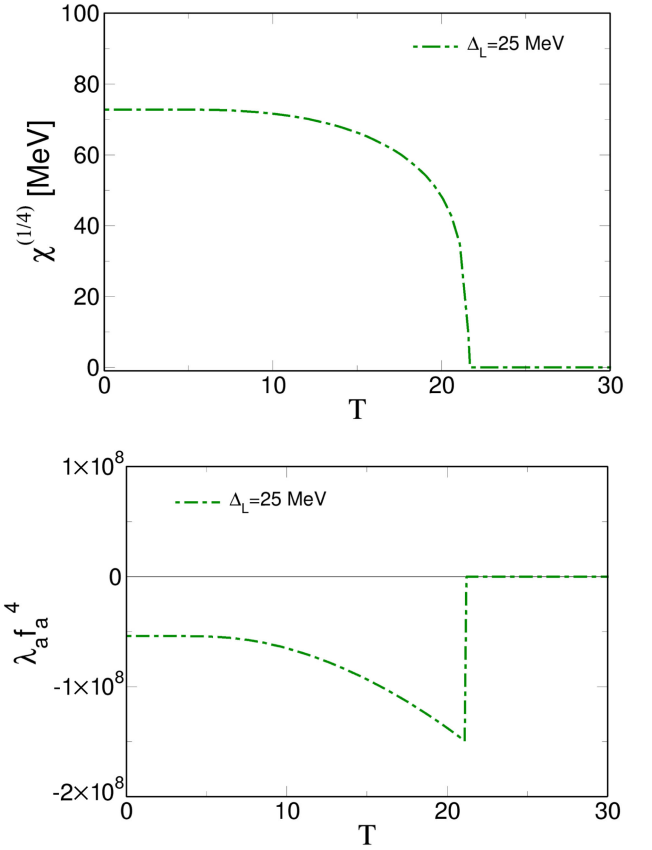


FIG. 9. Topological susceptibility, $\chi^{1/4}$ (upper panel) and axion self-coupling, $\lambda_a f_a^4$ (lower panel), versus T for $\zeta = 1$. We used $\mu = 400$ MeV, $\Lambda = 1000$ MeV, and $\Delta_L = 25$ MeV.

IV. CONCLUSIONS AND OUTLOOK

We analyzed the QCD axion potential in dense, superconductive quark matter at finite quark chemical potential, μ , and finite temperature, T . We assumed that both scalar, $\Delta_R - \Delta_L$, and pseudoscalar, $\Delta_R + \Delta_L$, diquark condensates can form: the color-flavor structure that we assume is that of the standard 2SC phase. We used a two-flavor model based on an interaction that contains a $U(1)_A$ -preserving and a $U(1)_A$ -breaking term: the former has coupling strength G_D and is assumed to be derived from one-gluon exchange; while the latter arises from the one-instanton exchange; it has coupling strength ζG_D , and contains the coupling of the QCD axion, a , to the quarks. We treated G_D and ζ as free parameters: in particular, we tuned G_D for a given ζ in order to reproduce a value of the superconductive gap without axions; we then switch on the axion field and study the response of the diquark condensate, as well as of the thermodynamic potential, to a . This allowed us to compute the axion potential in dense quark matter.

We found that for $a = 0$ and $\zeta > 0$ the scalar condensate is favored; however, increasing a/f_a in the range $(0, \pi/2)$ results in the global minima of Ω to become less shallow along the direction of the scalar condensate and in the

formation of new global minima around the direction of the pseudoscalar. Consequently, for a/f_a in the range $(\pi/2, 3\pi/2)$ the pseudoscalar condensate replaces the scalar one. Increasing further a/f_a up to 2π the location of the global minima of Ω change again and the system turns to condensate in the scalar channel.

We computed the full topological susceptibility, χ , of the 2SC phase, finding an analytical formula that connects χ to the quark condensate; this relation holds both at zero and at finite temperature. Our formula (52) explicitly contains information relative to the specific model used in our work, in particular, the effective coupling G_D and ζ . It is likely that in a more refined framework, in which one uses a momentum-dependent one-gluon exchange term and an instanton kernel instead of our effective 4-fermion interactions, both G_D and ζ will be replaced by quantities directly related to QCD, namely the QCD coupling, a dressed gluon mass as well as the instanton size. This interesting improvement will be the subject of a near future work. The introduction of the momentum-dependent gluon term would also allow us to explore the effect of cutting high momenta in the temperature dependent contribution to the thermodynamic potential, as we mentioned in Sec. II B.

We then computed the axion mass, m_a , which is related to χ by the relation $\chi = m_a^2 f_a^2$: as a consequence of our result (52), we were able to obtain an analytical formula for m_a in the 2SC phase of QCD. Also, in this case, it is our hope that the dependence of m_a on the parameters of our model can be replaced by a dependence on quantities of QCD by using more refined interactions instead of the 4-fermion terms we adopted here. We completed this part of the study by computing the axion self-coupling, λ_a . Interestingly, we found a range of ζ where $\lambda_a > 0$, differently from what was found in cases of normal quark matter; see for example [9,55,65–67,83]: hence the interaction among axions becomes repulsive in this range of ζ . This might have some impact on the pressure of axions trapped in the core of compact stellar objects. It will be interesting to explore this scenario in detail in the future.

A possible improvement of the present work is the inclusion of the strange quark, and the opening to the three-flavor color superconductor with massive quarks. This would potentially make the picture more complicated, because in this work we neglected the current quark masses, as well as light quark chiral condensate: previous studies based on NJL-like interactions show that this can be a fairly good approximation, as long as the light-quarks sector is considered. However, this might be no longer true for the strange quark, at least for the values of μ which are relevant for compact stars. Along this line, studying the axions in gapless phases is also worth more investigation: works in this direction are already ongoing, and we plan to report on them soon. Secondly, it would be interesting to use the results obtained here to compute the cooling of compact stellar objects via axion emission. It would also be important

to check how the picture we drew in our work changes when the local interaction kernels we used are replaced by nonlocal ones, with a more direct link to QCD, as well as when other interaction channels, in primis the vector and axial-vector channels are included in the game. Even more, it is of a certain interest to allow for chiral condensate besides the diquark one, in order to study, within a single model, the axion potential in proximity of the phase transition between the chiral and the superconductive phases: this would allow for the exploration of the properties of the axion in the whole QCD phase diagram. We leave all these interesting improvements to future works.

ACKNOWLEDGMENTS

M. R. acknowledges John Petrucci for inspiration. D. E. A. C. acknowledges support from the program Excellence Initiative–Research University of the University of Wrocław of the Ministry of Education and Science. A. G. G. would like to acknowledge the support received from CONICET (Argentina) under Grant No. PIP 22-24 11220210100150CO and from ANPCyT (Argentina) under Grant No. PICT20-01847. This work has been partly funded by the European Union—Next Generation EU through the research Grant No. P2022Z4P4B “SOPHYA—Sustainable Optimised PHYSics Algorithms: fundamental physics to build an advanced society” under the program PRIN 2022 PNRR of the Italian Ministero dell’Università e Ricerca (MUR).

APPENDIX A: HDET GAP EQUATION

In this section, we derive the HDET solution to the gap equation (41). To this end, we put

$$\Theta(a, \zeta) = \frac{A(a, \zeta)}{2 + \zeta \cos(a/f_a)}. \quad (\text{A1})$$

Then, Eq. (41) gives

$$1 = \frac{G_D}{2\pi^2} \Theta(a, \zeta) \int_0^\Lambda p^2 dp \left(\frac{1}{\sqrt{(p-\mu)^2 + G_D^2 h_L^2 A(a, \zeta)}} + \frac{1}{\sqrt{(p+\mu)^2 + G_D^2 h_L^2 A(a, \zeta)}} \right). \quad (\text{A2})$$

We then adopt the approximations of HDET [98]. Firstly, we note that the first integral on the right-hand side of (A2) gets its largest contribution from the momentum space region $p \approx \mu$, namely around the Fermi surface of the quarks. Moreover, the second integral in the right-hand side is suppressed at large μ in comparison with the first one, since it does not receive the enhancement for $p \approx \mu$. Within the spirit of HDET we can thus ignore the second integral, and restrict the first integral to a thin shell around $p = \mu$: we call δ the width of this shell. In the limit $\delta \ll \mu$ the

volume of momentum space available for pairing is thus $8\pi\mu^2\delta$. Introducing $\xi = p - \mu$, the HDET version of (A2) reads as¹

$$1 = \frac{G_D\mu^2}{2\pi^2} \Theta(a, \zeta) \int_{-\delta}^{+\delta} \frac{d\xi}{\sqrt{\xi^2 + G_D^2 h_L^2 A(a, \zeta)}}. \quad (\text{A3})$$

Integration can be done exactly; in the weak coupling limit $\delta \gg G_D h_L$, using the definition (39), we finally get

$$\Delta_L = \frac{4\delta}{\sqrt{A(a, \zeta)}} \exp\left(-\frac{\pi^2}{\mu^2 G_D \Theta(a, \zeta)}\right). \quad (\text{A4})$$

APPENDIX B: DERIVATION OF EQ. (52)

In this section, we derive Eq. (52) starting from Ω in (37) and using the gap equation (41). The first step in the calculation is to notice that all the results we found are

$$\chi = 8\zeta G_D h_L^2 \left[-\frac{1}{4} + \frac{G_D}{2\pi^2} \int_0^\Lambda p^2 dp \left(\frac{1}{\sqrt{(p-\mu)^2 + (2+\zeta)^2 G_D^2 h_L^2}} + \mu \rightarrow -\mu \right) \right]. \quad (\text{B3})$$

Now, we notice from the gap equation (41) at $\theta = 0$ that

$$\frac{1}{2+\zeta} = \frac{G_D}{2\pi^2} \int_0^\Lambda p^2 dp \left(\frac{1}{\sqrt{(p-\mu)^2 + (2+\zeta)^2 G_D^2 h_L^2}} + \mu \rightarrow -\mu \right), \quad (\text{B4})$$

where h_L stands for the condensate at $\theta = 0$. Using (B4) in (B3) we get

$$\chi = 2G_D h_L^2 \zeta \frac{2-\zeta}{2+\zeta}. \quad (\text{B5})$$

Finally, taking into account $\Delta_L = 2G_D h_L$ [see Eq. (39)] we have

$$\chi = \frac{\Delta_L^2}{2G_D} \zeta \frac{2-\zeta}{2+\zeta}, \quad (\text{B6})$$

in agreement with Eq. (52). We remark that Δ_L in (B6) denotes the diquark condensate at $\theta = 0$. From the

¹To be precise, in the HDET one introduces a sum over the direction of the Fermi velocities, \mathbf{v}_F , of the quarks; then, for each \mathbf{v}_F , $\xi = \mathbf{p} \cdot \mathbf{v}_F - \mu v_F$ measures the fluctuation of the longitudinal momentum around the Fermi surface. Our ξ in (A3) is slightly different from that of HDET; nevertheless, formally the gap equation obtained within HDET is in agreement with (A3), because the quark condensate is homogeneous and the sum over velocities leads to an overall 1.

consistent with the conditions $\partial\Omega/\Delta_L = \partial\Omega/\Delta_R = 0$ at $\theta = 0$ and at the minima of Ω . This can be easily understood since Ω develops minima along the directions $\Delta_L = \pm\Delta_R$, and on these lines, it is an even function of Δ_L or Δ_R . Hence we can write

$$\chi = \frac{d^2\Omega}{d\theta^2} \Big|_{\theta=0} = \frac{\partial^2\Omega}{\partial\theta^2} \Big|_{\theta=0}. \quad (\text{B1})$$

From Eq. (37) we get

$$\chi = 2\zeta G_D h_L h_R - \frac{1}{\pi^2} \int_0^\Lambda p^2 dp \frac{\partial^2}{\partial\theta^2} (\varepsilon_3 + \varepsilon_5 + \mu \rightarrow -\mu). \quad (\text{B2})$$

Along the line $h_L = -h_R$, which is the relevant one for small θ , and taking into account the expressions of the dispersion laws of the quarks, we thus get

derivation presented here, it is evident that Eq. (52) stands both at zero and at finite temperature, since the momentum integrals in Eqs. (B3) and (B4) are modified in the same fashion at $T \neq 0$.

As we remarked in the main text, for $\zeta < 0$ the role of the scalar and pseudoscalar condensates invert, since the minima of Ω develop along the line $h_L = h_R$ in this case, and Eq. (52) becomes

$$\chi = -\frac{\Delta_L^2}{2G_D} \zeta \frac{2+\zeta}{2-\zeta}. \quad (\text{B7})$$

Hence, we can summarize the results (52) and (B7) as

$$\chi = \frac{\Delta_L^2}{2G_D} |\zeta| \frac{2-|\zeta|}{2+|\zeta|}. \quad (\text{B8})$$

APPENDIX C: DERIVATION OF EQ. (56)

We consider the HDET gap equation Eq. (A3), and evaluate the integral analytically in the case $a = 0$ and $\delta \gg G_D h_L$ thus obtaining

$$1 = \frac{G_D \mu^2}{\pi^2} (2 + \zeta) \ln \left(\frac{4\delta}{G_D h_L^0 (2 + \zeta)} \right), \quad (\text{C1})$$

where h_L^0 is the value of the gap which satisfies the 0-temperature gap equation.

In the same framework, we now consider the finite temperature gap equation for $a = 0$, which can be written as

$$-1 + \frac{G_D \mu^2}{2\pi^2} (2 + \zeta) \int_{-\delta}^{+\delta} \frac{d\xi}{\sqrt{\xi^2 + G_D^2 h_L^2 (2 + \zeta)^2}} = \frac{G_D \mu^2}{2\pi^2} (2 + \zeta) \int_{-\delta}^{+\delta} \frac{d\xi}{\sqrt{\xi^2 + G_D^2 h_L^2 (2 + \zeta)^2 (1 + e^{\sqrt{G_D h_L (2 + \zeta)^2 + \xi^2}/T})}}. \quad (\text{C2})$$

The integral appearing on the left-hand side of the equation above is analogous to the one in Eq. (A3). Thus, the integration leads to the same result that appears in the rhs of Eq. (A1), with the only difference that h_L^0 is replaced by the finite temperature gap h_L . Inserting then Eq. (A1) into the lhs of Eq. (A2), and noticing that the fast convergence of the integral in the right-hand side of (C2) allows us to extend the integration to the whole real axis, we obtain

$$\begin{aligned} & \ln \left(\frac{h_L^0}{h_L} \right) \\ &= \int_{-\infty}^{+\infty} \frac{d\xi}{\sqrt{\xi^2 + G_D^2 h_L^2 (2 + \zeta)^2} (1 + e^{\sqrt{G_D h_L (2 + \zeta)^2 + \xi^2}/T})} \\ &\equiv I(u), \end{aligned} \quad (\text{C3})$$

where we put

$$I(u) = \int_{-\infty}^{+\infty} \frac{dx}{\sqrt{x^2 + u^2} (1 + e^{\sqrt{u^2 + x^2}})}, \quad (\text{C4})$$

with $x = \xi/T$ and $u = G_D h_L (2 + \zeta)/T$. For $T \rightarrow T_c$ the condensate $h_l \rightarrow 0$; we can thus limit ourselves to consider

the leading order expansion of Eq. (A4) for $u \sim 0$, namely

$$I(u)|_{u \rightarrow 0} \simeq \ln \left(\frac{\pi}{e^\gamma u} \right), \quad (\text{C5})$$

where $\gamma \approx 0.577$ is the Euler-Mascheroni constant. Using this result in Eq. (A3) we obtain

$$\ln \left(\frac{h_L^0}{h_L} \right) = \ln \left(\frac{\pi T_c}{\gamma G_D (2 + \zeta) h_L} \right), \quad (\text{C6})$$

where we set $T = T_c$ and discarded all the finite h_L^2 contributions. Finally, Eq. (A3) can be fulfilled only if

$$h_L^0 = \frac{\pi T_c}{\gamma G_D (2 + \zeta)}, \quad (\text{C7})$$

which gives from which we derive

$$T_c = \Delta_L^0 \frac{e^\gamma (2 + \zeta)}{2\pi}, \quad (\text{C8})$$

in agreement with (56).

-
- [1] R. D. Peccei and H. R. Quinn, *Phys. Rev. D* **16**, 1791 (1977).
 - [2] R. D. Peccei and H. R. Quinn, *Phys. Rev. Lett.* **38**, 1440 (1977).
 - [3] S. Weinberg, *Phys. Rev. Lett.* **40**, 223 (1978).
 - [4] F. Wilczek, *Phys. Rev. Lett.* **40**, 279 (1978).
 - [5] J. E. Kim and G. Carosi, *Rev. Mod. Phys.* **82**, 557 (2010); **91**, 049902(E) (2019).
 - [6] D. A. Easson, I. Sawicki, and A. Vikman, *J. Cosmol. Astropart. Phys.* **11** (2011) 021.
 - [7] E. Berkowitz, M. I. Buchoff, and E. Rinaldi, *Phys. Rev. D* **92**, 034507 (2015).
 - [8] A. Davidson and K. C. Wali, *Phys. Rev. Lett.* **48**, 11 (1982).
 - [9] G. Grilli di Cortona, E. Hardy, J. Pardo Vega, and G. Villadoro, *J. High Energy Phys.* **01** (2016) 034.
 - [10] L. D. Duffy and K. van Bibber, *New J. Phys.* **11**, 105008 (2009).
 - [11] M. S. Turner and F. Wilczek, *Phys. Rev. Lett.* **66**, 5 (1991).
 - [12] L. Visinelli and P. Gondolo, *Phys. Rev. D* **80**, 035024 (2009).
 - [13] P. Sikivie, *Phys. Rev. Lett.* **48**, 1156 (1982).
 - [14] J. Preskill, M. B. Wise, and F. Wilczek, *Phys. Lett.* **120B**, 127 (1983).
 - [15] L. F. Abbott and P. Sikivie, *Phys. Lett.* **120B**, 133 (1983).
 - [16] M. Dine and W. Fischler, *Phys. Lett.* **120B**, 137 (1983).
 - [17] J. E. Kim, *Phys. Rev. Lett.* **43**, 103 (1979).

- [18] M. A. Shifman, A. I. Vainshtein, and V. I. Zakharov, *Nucl. Phys.* **B166**, 493 (1980).
- [19] M. Dine, W. Fischler, and M. Srednicki, *Phys. Lett.* **104B**, 199 (1981).
- [20] A. Caputo and G. Raffelt, *Proc. Sci. COSMICWISPer* (2024) 041.
- [21] R. J. Crewther, P. Di Vecchia, G. Veneziano, and E. Witten, *Phys. Lett.* **88B**, 123 (1979).
- [22] C. A. Baker, D. D. Doyle, P. Geltenbort, K. Green, M. G. D. van der Grinten, P. G. Harris, P. Iaydjiev, S. N. Ivanov, D. J. R. May, J. M. Pendlebury *et al.*, *Phys. Rev. Lett.* **97**, 131801 (2006).
- [23] W. C. Griffith, M. D. Swallows, T. H. Loftus, M. V. Romalis, B. R. Heckel, and E. N. Fortson, *Phys. Rev. Lett.* **102**, 101601 (2009).
- [24] R. H. Parker, M. R. Dietrich, M. R. Kalita, N. D. Lemke, K. G. Bailey, M. Bishof, J. P. Greene, R. J. Holt, W. Korsch, Z. T. Lu *et al.*, *Phys. Rev. Lett.* **114**, 233002 (2015).
- [25] B. Graner, Y. Chen, E. G. Lindahl, and B. R. Heckel, *Phys. Rev. Lett.* **116**, 161601 (2016); **119**, 119901(E) (2017).
- [26] N. Yamanaka, T. Yamada, E. Hiyama, and Y. Funaki, *Phys. Rev. C* **95**, 065503 (2017).
- [27] F. K. Guo, R. Horsley, U. G. Meissner, Y. Nakamura, H. Perl, P. E. L. Rakow, G. Schierholz, A. Schiller, and J. M. Zanotti, *Phys. Rev. Lett.* **115**, 062001 (2015).
- [28] T. Bhattacharya, V. Cirigliano, R. Gupta, H. W. Lin, and B. Yoon, *Phys. Rev. Lett.* **115**, 212002 (2015).
- [29] M. Colpi, S. L. Shapiro, and I. Wasserman, *Phys. Rev. Lett.* **57**, 2485 (1986).
- [30] I. I. Tkachev, *Phys. Lett. B* **261**, 289 (1991).
- [31] E. W. Kolb and I. I. Tkachev, *Phys. Rev. Lett.* **71**, 3051 (1993).
- [32] P. H. Chavanis, *Phys. Rev. D* **84**, 043531 (2011).
- [33] F. S. Guzman and L. A. Urena-Lopez, *Astrophys. J.* **645**, 814 (2006).
- [34] J. Barranco and A. Bernal, *Phys. Rev. D* **83**, 043525 (2011).
- [35] E. Braaten, A. Mohapatra, and H. Zhang, *Phys. Rev. Lett.* **117**, 121801 (2016).
- [36] S. Davidson and T. Schwetz, *Phys. Rev. D* **93**, 123509 (2016).
- [37] J. Eby, M. Leembruggen, P. Suranyi, and L. C. R. Wijewardhana, *J. High Energy Phys.* **12** (2016) 066.
- [38] T. Helfer, D. Marsh, K. Clough, M. Fairbairn, E. Lim, and R. Becerril, *J. Cosmol. Astropart. Phys.* **03** (2017) 055.
- [39] D. G. Levkov, A. G. Panin, and I. I. Tkachev, *Phys. Rev. Lett.* **118**, 011301 (2017).
- [40] J. Eby, M. Leembruggen, P. Suranyi, and L. C. R. Wijewardhana, *J. High Energy Phys.* **06** (2017) 014.
- [41] L. Visinelli, S. Baum, J. Redondo, K. Freese, and F. Wilczek, *Phys. Lett. B* **777**, 64 (2018).
- [42] P. H. Chavanis, *Phys. Rev. D* **94**, 083007 (2016).
- [43] E. Cotner, *Phys. Rev. D* **94**, 063503 (2016).
- [44] Y. Bai, V. Barger, and J. Berger, *J. High Energy Phys.* **12** (2016) 127.
- [45] P. Sikivie and Q. Yang, *Phys. Rev. Lett.* **103**, 111301 (2009).
- [46] P. H. Chavanis, *Phys. Rev. D* **98**, 023009 (2018).
- [47] R. Balkin, J. Serra, K. Springmann, S. Stelzl, and A. Weiler, *Phys. Rev. D* **109**, 095032 (2024).
- [48] R. Balkin, J. Serra, K. Springmann, S. Stelzl, and A. Weiler, *arXiv:2307.14418*.
- [49] J. W. Wang, X. J. Bi, R. M. Yao, and P. F. Yin, *Phys. Rev. D* **103**, 115021 (2021).
- [50] F. Calore, P. Carena, C. Eckner, T. Fischer, M. Giannotti, J. Jaeckel, K. Kotake, T. Kuroda, A. Mirizzi, and F. Sivo, *Phys. Rev. D* **105**, 063028 (2022).
- [51] A. Sedrakian, *Phys. Rev. D* **93**, 065044 (2016).
- [52] L. B. Leinson, *J. Cosmol. Astropart. Phys.* **08** (2014) 031.
- [53] A. Sedrakian, *Phys. Rev. D* **99**, 043011 (2019).
- [54] M. Buschmann, C. Dessert, J. W. Foster, A. J. Long, and B. R. Safdi, *Phys. Rev. Lett.* **128**, 091102 (2022).
- [55] B. S. Lopes, R. L. S. Farias, V. Dexheimer, A. Bandyopadhyay, and R. O. Ramos, *Phys. Rev. D* **106**, L121301 (2022).
- [56] C. H. Lenzi, M. Dutra, O. Lourenço, L. L. Lopes, and D. P. Menezes, *Eur. Phys. J. C* **83**, 266 (2023).
- [57] G. Lucente, P. Carena, T. Fischer, M. Giannotti, and A. Mirizzi, *J. Cosmol. Astropart. Phys.* **12** (2020) 008.
- [58] T. Fischer, P. Carena, B. Fore, M. Giannotti, A. Mirizzi, and S. Reddy, *Phys. Rev. D* **104**, 103012 (2021).
- [59] Y. Nambu and G. Jona-Lasinio, *Phys. Rev.* **122**, 345 (1961).
- [60] M. Buballa, *Phys. Rep.* **407**, 205 (2005).
- [61] S. P. Klevansky, *Rev. Mod. Phys.* **64**, 649 (1992).
- [62] T. Hatsuda and T. Kunihiro, *Phys. Rep.* **247**, 221 (1994).
- [63] S. B. Ruester, V. Werth, M. Buballa, I. A. Shovkovy, and D. H. Rischke, *Phys. Rev. D* **72**, 034004 (2005).
- [64] D. Blaschke, S. Fredriksson, H. Grigorian, A. M. Oztas, and F. Sandin, *Phys. Rev. D* **72**, 065020 (2005).
- [65] Z. Y. Lu and M. Ruggieri, *Phys. Rev. D* **100**, 014013 (2019).
- [66] A. Bandyopadhyay, R. L. S. Farias, B. S. Lopes, and R. O. Ramos, *Phys. Rev. D* **100**, 076021 (2019).
- [67] A. Das, H. Mishra, and R. K. Mohapatra, *Phys. Rev. D* **103**, 074003 (2021).
- [68] R. K. Mohapatra, A. Abhishek, A. Das, and H. Mishra, *Springer Proc. Phys.* **277**, 455 (2022).
- [69] Y. Nambu and G. Jona-Lasinio, *Phys. Rev.* **124**, 246 (1961).
- [70] M. G. Alford, A. Schmitt, K. Rajagopal, and T. Schäfer, *Rev. Mod. Phys.* **80**, 1455 (2008).
- [71] I. A. Shovkovy, *Found. Phys.* **35**, 1309 (2005).
- [72] R. Rapp, T. Schäfer, E. V. Shuryak, and M. Velkovsky, *Ann. Phys. (N.Y.)* **280**, 35 (2000).
- [73] R. Rapp, T. Schäfer, E. V. Shuryak, and M. Velkovsky, *Phys. Rev. Lett.* **81**, 53 (1998).
- [74] R. Brower, S. Chandrasekharan, J. W. Negele, and U. J. Wiese, *Phys. Lett. B* **560**, 64 (2003).
- [75] Y. Y. Mao and T.-W. Chiu (TWQCD Collaboration), *Phys. Rev. D* **80**, 034502 (2009).
- [76] S. Aoki and H. Fukaya, *Phys. Rev. D* **81**, 034022 (2010).
- [77] V. Bernard, S. Descotes-Genon, and G. Toucas, *J. High Energy Phys.* **12** (2012) 080.
- [78] V. Bernard, S. Descotes-Genon, and G. Toucas, *J. High Energy Phys.* **06** (2012) 051.
- [79] M. A. Melitski and A. R. Zhitnitsky, *Phys. Lett. B* **633**, 721 (2006).

- [80] S. Borsanyi, Z. Fodor, J. Guenther, K. H. Kampert, S. D. Katz, T. Kawanai, T. G. Kovacs, S. W. Mages, A. Pasztor, F. Pittler *et al.*, *Nature (London)* **539**, 69 (2016).
- [81] S. Aoki *et al.* (JLQCD Collaboration), *EPJ Web Conf.* **175**, 04008 (2018).
- [82] C. Bonati, M. D’Elia, M. Mariti, G. Martinelli, M. Mesiti, F. Negro, F. Sanfilippo, and G. Villadoro, *J. High Energy Phys.* **03** (2016) 155.
- [83] B. Zhang, D. E. A. Castillo, A. G. Grunfeld, and M. Ruggieri, *Phys. Rev. D* **108**, 054010 (2023).
- [84] H. F. Gong, Q. Lu, Z. Y. Lu, L. M. Liu, X. Chen, and S. P. Wang, [arXiv:2404.15136](https://arxiv.org/abs/2404.15136).
- [85] A. Davidson and M. A. H. Vozmediano, *Nucl. Phys.* **B248**, 647 (1984).
- [86] A. Davidson and M. A. H. Vozmediano, *Phys. Lett.* **141B**, 177 (1984).
- [87] G. Gabadadze and M. A. Shifman, *Phys. Rev. D* **62**, 114003 (2000).
- [88] F. Takahashi, W. Yin, and A. H. Guth, *Phys. Rev. D* **98**, 015042 (2018).
- [89] R. L. Workman *et al.* (Particle Data Group), *Prog. Theor. Exp. Phys.* **2022**, 083C01 (2022).
- [90] Y. Nagashima, *Beyond the Standard Model of Elementary Particle Physics* (Wiley-VCH, New York, 2014), ISBN 978-3-527-41177-1, 978-3-527-66505-1.
- [91] M. Shifman, *Advanced Topics in Quantum Field Theory* (Cambridge University Press, Cambridge, England, 2022), ISBN 978-1-108-88591-1, 978-1-108-84042-2.
- [92] R. Balkin, J. Serra, K. Springmann, and A. Weiler, *J. High Energy Phys.* **07** (2020) 221.
- [93] G. ’t Hooft, *Phys. Rev. D* **14**, 3432 (1976); **18**, 2199(E) (1978).
- [94] G. ’t Hooft, *Phys. Rep.* **142**, 357 (1986).
- [95] C. Ratti, M. A. Thaler, and W. Weise, *Phys. Rev. D* **73**, 014019 (2006).
- [96] C. Ratti and W. Weise, *Phys. Rev. D* **70**, 054013 (2004).
- [97] M. Ruggieri and G. X. Peng, *J. Phys. G* **43**, 125101 (2016).
- [98] G. Nardulli, *Riv. Nuovo Cimento* **25N3**, 1 (2002).
- [99] J. Bardeen, L. N. Cooper, and J. R. Schrieffer, *Phys. Rev.* **106**, 162 (1957).
- [100] J. Bardeen, L. N. Cooper, and J. R. Schrieffer, *Phys. Rev.* **108**, 1175 (1957).
- [101] R. Gatto and M. Ruggieri, *Phys. Rev. D* **85**, 054013 (2012).
- [102] G. Veneziano, *Nucl. Phys.* **B159**, 213 (1979).
- [103] P. Di Vecchia and G. Veneziano, *Nucl. Phys.* **B171**, 253 (1980).
- [104] R. J. Crewther, *Phys. Lett.* **70B**, 349 (1977).
- [105] H. Leutwyler and A. V. Smilga, *Phys. Rev. D* **46**, 5607 (1992).